ACADEMIA ROMÂNĂ
Revue Roumaine de Chimie
http://web.icf.ro/rrch/

Rev. Roum. Chim.,
2018, *63*(10), 911-918

COWHIDE COLLAGEN FIBERS AS BIOTEMPLATES FOR PREPARATION OF FIBROUS SO_4^{2-}/ZrO_2-NiO SOLID ACID CATALYST AND THEIR APPLICATION IN ESTERIFICATION

Yang LIAO,[a,b] Yunfei QIU,[a] Yujia WANG,[a] Ting ZHANG,[a] Xin FENG,[a] Hongyan SHANG,[a,b] Shilin ZHAO,[a,b] Jun MA[a,b] and Hui MAO*[a,b]

[a] College of Chemistry and Materials Science, Sichuan Normal University, Chengdu 610068, P. R. China
[b] Key Laboratory of Land Resources Evaluation and Monitoring in Southwest, Sichuan Normal University, Ministry of Education, Chengdu 610068, PR China

Received October 20, 2017

Cowhide collagen fibers were used as biotemplates to prepare a series of fibrous SO_4^{2-}/ZrO_2-NiO solid acid catalysts. The as-prepared catalysts were characterized by scanning electron microscopy (SEM), X-ray diffraction (XRD), N_2 adsorption/desorption isotherms and the temperature-programmed decomposition (TPD), respectively. The characterization suggested that the SO_4^{2-}/ZrO_2-NiO catalysts have well-defined fibrous morphology which maintains the fibrous structure of cowhide collagen fibers. TPD of ammonia indicated that the catalyst had both medium strong acidic sites and strong acidic sites. The esterification of acetic acid with n-butanol was utilized as model reaction to evaluate the catalytic performance of the catalysts. The catalyst has exhibited high catalytic activity and good reusability.

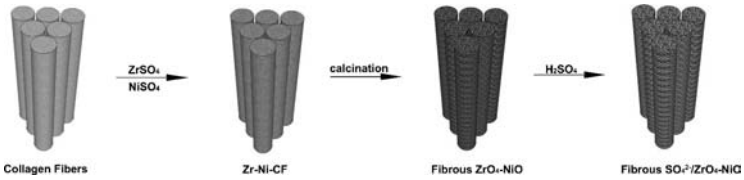

INTRODUCTION

The past few decades have witnessed a huge development in chemical industry owing to some effective acid catalysts being employed. Conventional homogeneous acid catalysts occupied a significant position in synthetic application and organic reactions, including alkylation, cracking, isomerization, esterification, acylation, etc.[1-3] However, the large scale application of the conventional liquid acid catalysts usually resulted in serious environment pollution for the problems of difficult recovery and apparatus corrosion, which decided by its homogeneous nature.[4-6] To solve these problems, the rational development of recyclable solid acids catalysts have been established as benign alternatives.[7-9] Among these solid acids catalysts, SO_4^{2-}/ZrO_2 and modified SO_4^{2-}/ZrO_2 solid acid catalysts have attracted considerable interests due to their strong acidity and catalytic activity, and have been widely used to catalyze various types of reactions.[10,11] However, its fast deactivation has prevented its application in commercial processes.[12] To solve this problem, the solid acid catalysts using mixed oxides as support often show enhanced acidity in comparison to the one using single metal oxides.[13,14] Mixing of two oxides may modulate the properties of the component oxides or generate new active sites by the bridged hetero metal-oxygen bonds between two oxides.[15] To realize the uniform distribution of two oxides and controlled the corresponding pore size of the mixed oxides is still a challenge. Recently, template technique has emerged as promising strategy for the effective and convenient fabrication of inorganic porous supports.[16,17] By using porous matrices with ordered shape the templates can easily synthesize porous supports with highly

* Corresponding author: rejoice222@163.com

ordered structure.[18,19] However, the synthesis of organic template is often complicated, and toxic solvents may also be involved.[20] An environmentally benign alternative is to utilize natural polymer to replace the synthetic counterpart.

Cowhide collagen fiber is an abundant natural biomass which has the features of highly ordered arrangement, abundant functional groups, wide source and low cost.[21] The functional groups such as –OH,-COOH and $–NH_2$ could form a complex with the transition metal ions including Zr, Ni, Fe, etc.[22] Furthermore, the fibrous structure of CF could enhance the mass transfer during the reaction.[23] In previous studies of our group, we successfully prepared the porous ZrO_2 with fibrous morphology using cowhide collagen fiber as template.[24] In this work, we prepared a fibrous ZrO_2-NiO matrix using cowhide collagen fiber as template. Based on this, a fibrous SO_4^{2-}/ZrO_2-NiO solid acid was prepared. The surface morphology, acid strength, crystalline phases and structural properties of the as-prepared catalyst were investigated by a series of physical characterizations. The functional groups of CF could be beneficial for the uniform distribution of two oxides which could enhance the acidity, exhibiting high reactivity and stability.

EXPERIMENTAL

1. Materials

Collagen fiber was acquired from cattle skin according to our previous work. Zirconium sulfate, acetic acid, n-butanol, other reagents were offered by a commercial supplier (Chengdu Kelon Chemical Reagent Factory, China). The reagents and chemicals were all analytical grade reagents, and the water was deionized water.

2. Catalyst preparation

2.1. Preparation of fibrous ZrO_2-NiO

The preparation of collagen fiber method is according to our previous work. The detailed preparation procedure of ZrO_2-NiO was as follows: 7.5 g of collagen fiber was added into the three-necked bottle with 3 g/200 mL of NaCl solution at 25 ^oC for 2.0 h. Then H_2SO_4–HCOOH solution (H_2SO_4: HCOOH = 10:1, v/v) was added into the solution to adjust the pH value between 1.8 and 2.0, and the mixture was stirred with 150 rpm at 25 °C for 2.0 h. 15.0 g of $Zr(SO_4)_2$ and different amounts of $NiSO_4$ (0.1 g, 0.5 g, 1 g, 2 g, 4 g) were added. After that, the mixture was continued to be stirred at 25 °C and 350 rpm for 4.0 h, and the pH of the mixture was increased gradually to 4.0 and 4.2 within 3.0 h by adding dropwise a determined amount of $NaHCO_3$ solution under stirring. After the system reached the desired pH value, the temperature of system was heated and kept at 45 °C under constant stirring for another 12.0 h. Then, the Zr-Ni-immobilized collagen fiber was collected by filtration, washing and drying at 45 °C. In order to remove the collagen fiber template, the obtained Zr-Ni-immobilized collagen fiber was treated by temperature-programmed calcination with temperature from 450 °C to 800 °C.

2.2. Preparation of fibrous SO_4^{2-}/ZrO_2-NiO

The fibrous 0.5g ZrO_2-NiO was impregnated into 20mL H_2SO_4 solution with different concentrations for 10.0 h (0.1M, 0.5M, 1.0M, 2.0M, 5.0M), and then collected by filtration. After drying, the product was calcinated for 4.0 h under 300 °C. At last, the sulfated ZrO_2-NiO was obtained.

3. Catalyst characterizations

The surface morphology of catalyst was characterized using a Scanning Electron Microscopy (SEM, JEOL LTDJSM-5900LV, Japan). The samples were sputtered with gold to reduce the influence of charging before testing. The specific surface areas and pore diameter of the catalysts were measured by N_2 adsorption–desorption isotherms method (Micromeritics TriStar Surface Area and Pority Analyzer, nitrogen absorption apparatus).X-ray diffraction (XRD) patterns of ZrO_2-NiO and SO_4^{2-}/ZrO_2-NiO were obtained from a Philips X'Pert ProMPD diffractometer (Netherlands) using Cu-Kα radiation source (λ=0.15406nm) with scanning angle ranging from 10 to 80° and the operating conditions were 40 KV and 25 mA. TGA analysis of catalyst was performed with TGAQ500. The heating rate and air velocity is 10°C/min and 50 mL/min, respectively. The acidity of sample was measured by NH_3-temperature programmed desorption using CHEMBET-Palsar TPR/TPD instrument equipped with TCD. About 0.5 g of catalyst was heated at a rate of 20 °C /min up to 200 °C and kept for 0.5 h in flow of N_2 gas (60 mL/min). Then the sample cooled to room temperature in a flow of the He gas and followed by adsorption of NH_3 gas flow, the NH_3-TPD data was recorded from 100 ◦C to 800 °C with a rate of 20 °C /min.

4. Catalytic reaction

Esterification of acetic acid with n-butanol was applied to evaluate the activities of the fibrous SO_4^{2-}/ZrO_2-NiO solid acid catalyst. The catalyst, acetic acid and *n*-butanol were put in a three necked bottle equipped with a reflux condenser. The reaction system was conducted at a certain temperature under constant stirring. After reaction finished, the reaction mixture was filtered, and the products were analyzed by means of gas chromatograph. Dichloromethane was added into the reaction system as an internal standard, and the area normalization method was introduced to estimate the conversion of n-butyl acetate. As for the reuse of experiments of catalyst, it was performed under the same reaction conditions described above.

RESULTS AND DISCUSSION

1. Catalyst characterization

1.1. The surface morphology of ZrO_2-NiO

The SEM image of pure collagen fiber (CF) is presented in Fig.1a. The CF still has well-defined fibrous morphology after reacting with Zr and Ni ions, as shown in Fig. 1b. Similar fibrous morphology can still be observed after calcination (Fig. 1c), in which nanoscaled ZrO_2 fibers are well arranged with defined fiber bundles. The morphology of the cowhide collagen fiber template was well preserved in prepared ZrO_2-NiO material. More importantly, the fibrous morphology can still be maintained after the treatment of sulfuric acid impregnation (Fig. 1d).

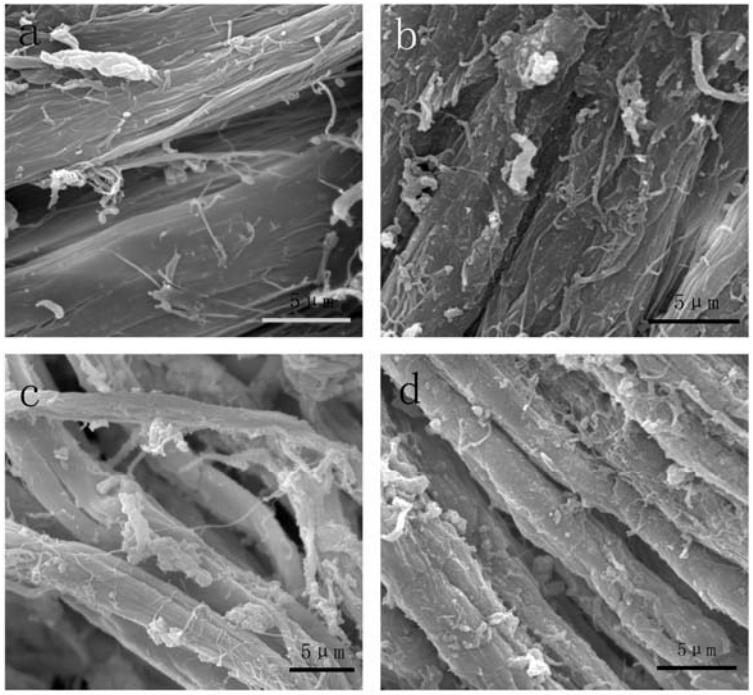

Fig. 1 – SEM images (a) pure collagen fiber (CF); (b) collagen fibers react with Zr and Ni ions; (c) fibrous ZrO_2-NiO calcined at 550 °C; (d) SO_4^{2-}/ZrO_2-NiO.

1.2. XRD characterization of ZrO_2-NiO

The X-ray diffraction patterns of ZrO_2-NiO with different amount of $Ni(NO_3)_2$ was shown in Fig. 2a. No diffraction peaks of nickel oxide and nickel zirconium composite oxide were observed, which may be due to less doped nickel ions and the high dispersion of NiO on the surface of the ZrO_2 crystals.[25] The crystal structure of ZrO_2-NiO prepared by adding 0.1 g, 0.5 g, 1.0 g and 2.0 g of nickel nitrate was only tetragonal phase of ZrO_2.[26] When the addition amount of nickel nitrate is 4.0 g, the ZrO_2 monoclinic crystal diffraction peak appears, indicating the existence of monoclinic phase structure.[27]

Fig. 2b shows the XRD patterns of ZrO_2-NiO prepared at different calcination temperatures. When the calcination temperature was from 450 °C to 600 °C, only tetragonal phase ZrO_2 was observed. Once the temperature reached 700 °C, the amount of monoclinic ZrO_2 phase increased clearly. When the calcination temperature reaches 800 °C, there is almost no tetragonal phase in the sample, which is consistent with the pure ZrO_2 transformation from tetragonal phase to monoclinic phase. No crystal diffraction peak of NiO was observed in the whole XRD pattern, which may be attributed to the highly uniform dispersion of doped Ni ions on the surface of ZrO_2 crystal.

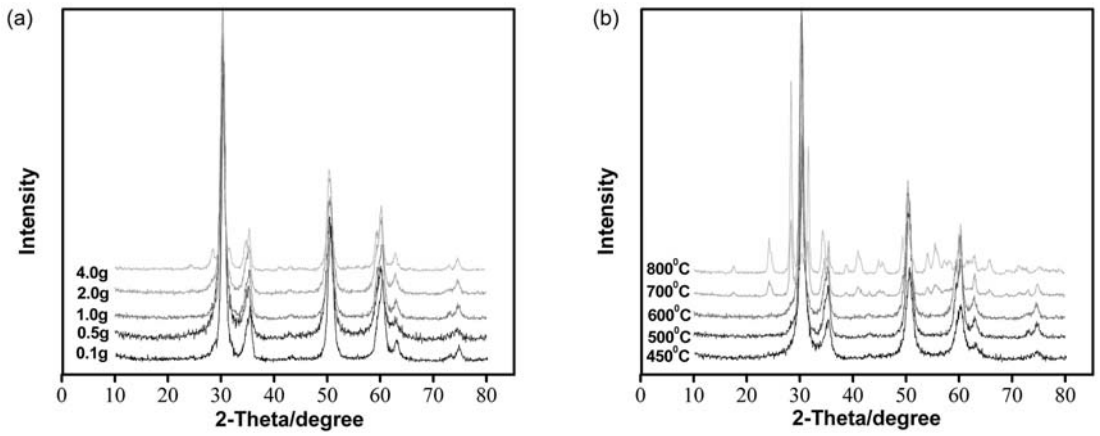

Fig. 2 – XRD characterization of ZrO_2-NiO. (a) XRD patterns of ZrO_2-NiO at different adding quality of $Ni(NO_3)_2$. (b) XRD patterns of ZrO_2-NiO prepared at different calcination temperatures.

1.3. N_2 adsorption/desorption and specific surface area

Fig. 3a shows the N_2 adsorption/desorption isotherms of ZrO_2-NiO prepared at different adding quality of $Ni(NO_3)_2$ (0.1 g, 0.5 g, 1.0 g, 2.0 g, 4.0 g). The curves of ZrO_2-NiO prepared by the addition of $Ni(NO_3)_2$ are in accordance with the adsorption and desorption isotherms and have H1 hysteresis loop, which indicates that ZrO_2-NiO fibers have mesoporous structure.[28] Simultaneously, the hysteresis band is almost the same, indicating that the mesopore diameter is uniform.[29] The N_2 adsorption-desorption isotherm analysis shows that the addition of nickel nitrate does not affect the mesoporous structure of ZrO_2.

Fig. 3b illustrates the pore size distribution of ZrO_2-NiO prepared at different adding quality of $Ni(NO_3)_2$ (0.1 g, 0.5 g, 1.0 g, 2.0 g, 4.0 g). Table 1 lists the average pore size of ZrO_2-NiO at different adding quality of $Ni(NO_3)_2$. The pore size distribution curve of ZrO_2-NiO prepared by $Ni(NO_3)_2$ is a narrow and sharp peak with narrow pore size distribution. The average pore size of ZrO_2-NiO is 8.07 nm, 7.61 nm, 9.88 nm, 11.19 nm and 12.48 nm, respectively. However, the average pore size of ZrO_2 without nickel nitrate is 16.2 nm, which indicated that the addition of nickel nitrate reduced the mesopore diameter of the catalyst. These results showed that the addition of nickel inhibits the aggregation of ZrO_2-NiO, maintains its mesoporous structure, and can improve the pore size distribution of ZrO_2, so that the pore structure is uniform and regular.

Basically, the specific surface area of the catalyst has significant influence on its catalytic activity.[30] Based on N_2 adsorption/desorption analysis, Table 2 summarizes specific surface area and pore volume of ZrO_2-NiO at different adding quality of $Ni(NO_3)_2$. The specific surface area and pore volume of ZrO_2-NiO firstly increased and then decreased with the addition of $Ni(NO_3)_2$. The BET surface area and pore volume of ZrO_2-NiO were 60.51m^2/g and 0.1335 cm^3/g when the addition amount of nickel nitrate was 1.0 g. Thereafter, the BET specific surface area and pore volume of ZrO_2-NiO gradually decreased with the addition of nickel. When the addition amount of nickel nitrate is 4.0 g, the specific surface area of ZrO_2-NiO decreases to 19.58 m^2/g and the pore volume is 0.05478 cm^3/g. Compared with pure ZrO_2 prepared under the same conditions, ZrO_2-NiO prepared by adding 0.1g, 0.5g, 1.0g and 2.0g nickel nitrate have higher BET surface area and pore volume than pure ZrO_2. In addition, the BJH surface area of ZrO_2-NiO is larger than the BET surface area, indicating that there is almost no microporous structure in the ZrO_2-NiO fiber. Combining the data of specific surface area and pore size, it is advisable to add 1.0 g of nickel nitrate.

By using the similar method, the effects of calcination temperature on the specific surface area and pore structure of ZrO_2-NiO fibers were investigated (Supplementary Fig. S1, S2 and Table S1). When the calcination temperature was 450 °C, the BET surface area of the samples was 66.03m^2/g, which was the highest among all the samples. With the calcination temperature rising from 450 °C to 800 °C, the BET surface area decreased from 66.03m^2/g to 4.63 m^2/g. However, the color of ZrO_2-NiO prepared at 450 ^oC is a little grey, which illuminated that the collagen fiber was not completely removed. As confirmed from XRD analysis and specific surface area analysis, 500 °C is suitable for preparation temperature of fibrous ZrO_2-NiO.

Table 1

Average pore diameter of ZrO_2-NiO at different adding quality of $Ni(NO_3)_2$

adding quality	0.1g	0.5g	1.0g	2.0g	4.0g
pore diameter(nm)	8.07	7.61	9.88	11.19	12.48

Table 2

Specific surface area and pore volume of ZrO_2-NiO at different adding quality of $Ni(NO_3)_2$

Sample	BET surface area (m^2/g)	BJH surface area (m^2/g)	Pore volume (cm^3/g)
0.1g $Ni(NO_3)_2$	40.17	48.41	0.08106
0.5g $Ni(NO_3)_2$	45.88	57.84	0.08735
1.0g $Ni(NO_3)_2$	60.51	78.43	0.1335
2.0g $Ni(NO_3)_2$	42.79	54.15	0.1107
4.0g $Ni(NO_3)_2$	19.58	27.83	0.05478

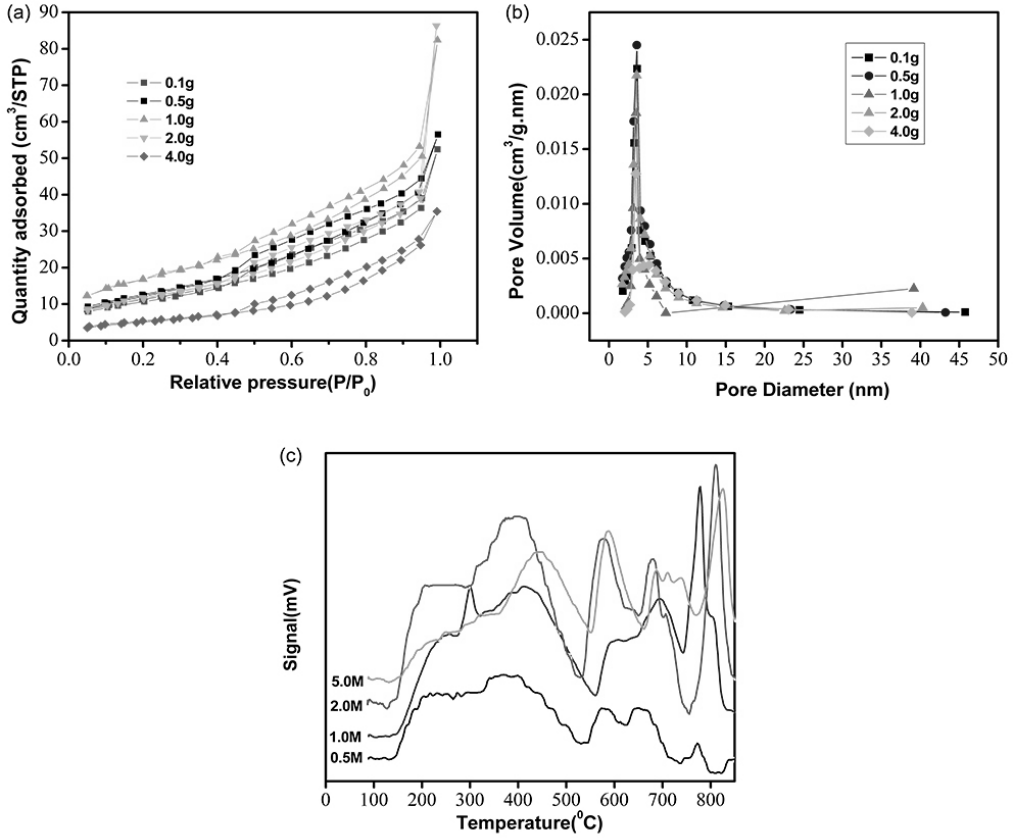

Fig. 3 – (a) N_2 adsorption-desorption isotherms of ZrO_2-NiO prepared at different adding quality of $Ni(NO_3)_2$: 0.1g, 0.5g, 1.0g, 2.0g, 4.0g. (b) Pore size distribution curves of ZrO_2-NiO prepared at different adding quality of $Ni(NO_3)_2$: 0.1g, 0.5g, 1.0g, 2.0g, 4.0g. (c) NH_3 – TPD curves of SO_4^{2-}/ ZrO_2-NiO prepared at different acid concentration.

1.4. NH_3-TPD analysis

The acid strength of sulfate groups deposited on the surface of SO_4^{2-}/ZrO_2-NiO was measured by temperature-programmed desorption (TPD). The NH_3-TPD curves of SO_4^{2-}/ ZrO_2-NiO prepared at different acid concentration are illustrated in Fig. 3c. The desorption temperature presents the acid strength of SO_4^{2-}/ZrO_2-NiO. The higher temperature of desorption means the stronger the acid strength. The desorption peaks of NH_3 were observed at a temperature between 150 °C and 500 °C when impregnating the concentration of sulfuric acid was 0.5M. Along with the increase of impregnating acid concentration, the peak signal from 150 °C to 500 °C heightened gradually, and the area of desorption peaks increased obviously, which indicated that the medium-strength acid sites in SO_4^{2-}/ZrO_2-NiO were strengthened with the increase of impregnating acid concentration. When the concentration of sulfuric acid was 1.0M, 2.0M, 5.0M, the intense desorption peaks were detected at a temperature between 600 °C and 800 °C, which attributes to strong acid sites, and intensity of the peak increases with the boost of the acid concentration. However, once the acid concentration reached 5.0M, the peak of medium strong acidic sites gradually broadened due to the excess SO_4^{2-} form overlapping structure covering the acid sites of the catalyst surface and the number of acidic sites decreases, which is leading to change in catalyst acidity. In general, the NH_3-desorption for two serials of SO_4^{2-}/ZrO_2-NiO took place at 150-500 ^oC and 600-800 ^oC, which suggested that the catalyst contains both medium-strength acid sites and strong acid sites.

On the other hand, the sulfur content of the catalysts is a pivotal factor for the acidity of the samples, which may greatly affect the catalytic activity. Table 3 exhibits the sulfur content of SO_4^{2-}/ZrO_2-NiO based on the TG curves of SO_4^{2-}/ZrO_2-NiO prepared at the different acid concentration (Supplementary Fig. S3). According to the literature, when the sulfur content of SO_4^{2-}/ZrO_2-NiO is 1.5% -3.0%, the catalyst has a high catalytic activity. Hence, incorporating with the NH_3-TPD analysis, it is reasonable that the impregnating acid concentration of samples is 2.0M.

Table 3

Sulfur content of SO_4^{2-}/ZrO_2-NiO prepared at different acid concentrations

acid concentration	0.1M	0.5M	1.0M	2.0M	5.0M
Sulfur content ($_{wt}$%)	0.03	0.93	1.33	2.58	13.75

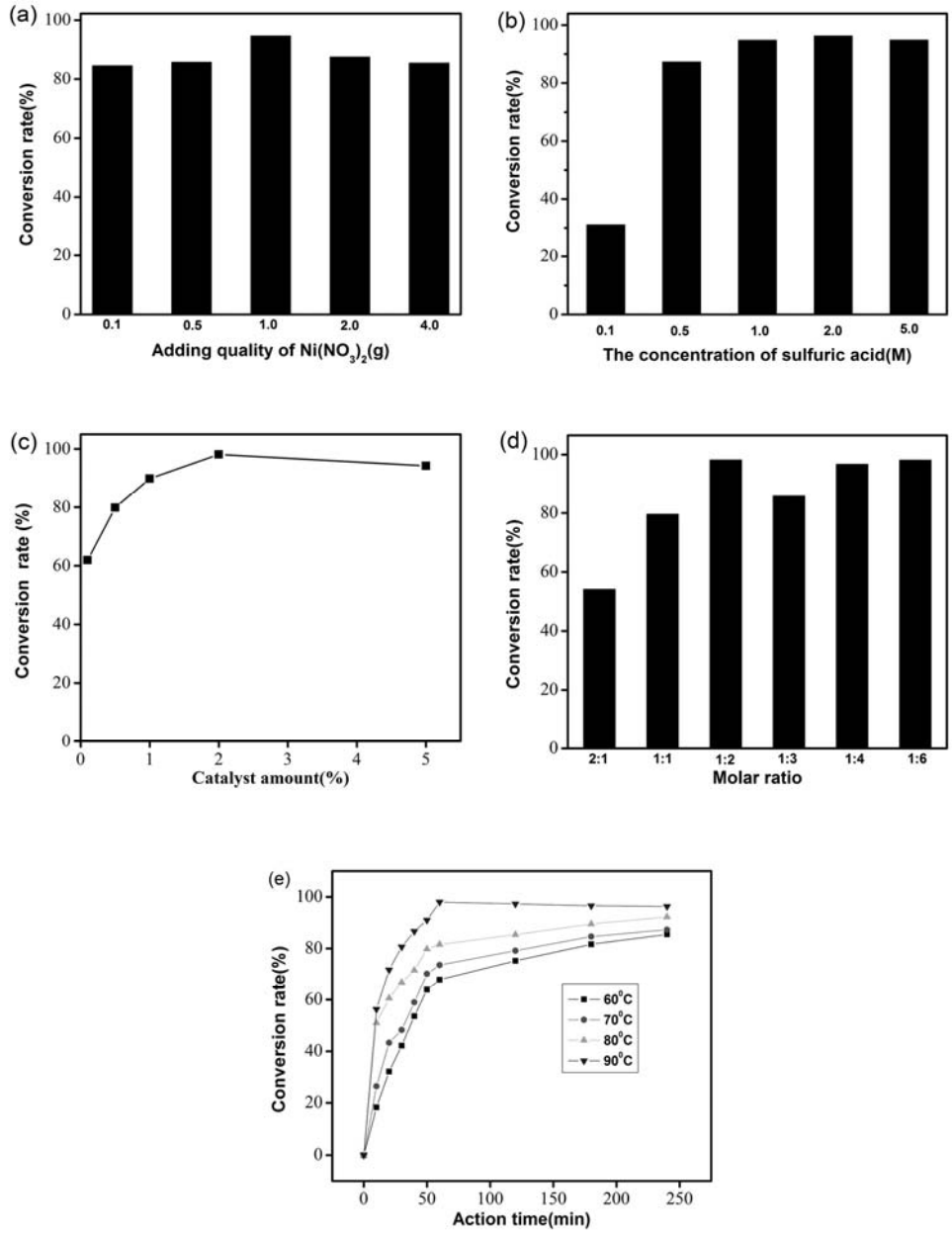

Fig. 4 – Catalytic activity of SO_4^{2-}/ZrO_2-NiO catalyst. (a)Effect of SO_4^{2-}/ZrO_2-NiO prepared at different adding quality of $Ni(NO_3)_2$ on the conversion rate of acetic acid. (b) Effect of SO_4^{2-}/ZrO_2-NiO prepared at different acid concentration on the conversion rate of acetic acid. (c) Effect of catalyst amount. (d) Effect of molar ratio of n-butanol to acetic acid on the conversion rate of acetic acid. (e) Effect of reaction temperature on esterification.

2. Catalytic activity

2.1. Effect of adding quality of $Ni(NO_3)_2$

The influence of SO_4^{2-}/ZrO_2-NiO prepared at different adding quality of $Ni(NO_3)_2$ on activity is shown in Fig. 4a. The condition of reaction is temperature at 90 °C, a certain acetic acid to n-butanol ratio of 1:2 for 1h, the impregnating acid concentration of samples is 1.0M and the amounts of catalyst is the quality of acetic acid 5%. The consequence expounded that the conversion increased with a change of $Ni(NO_3)_2$ adding from 0.1g to 1.0g. Along with further increase of $Ni(NO_3)_2$ adding from 1.0g to 4.0g, a markedly decrease in

conversion was observed. When the amount of $Ni(NO_3)_2$ was 1.0 g, the esterification rate of n-butyl acetate reached 95%, which is consistent with the previous analysis of specific surface area and pore size distribution. When the $Ni(NO_3)_2$ adding was 1.0g, the sample has the highest specific surface area and the largest pore size, meanwhile, the plentiful acid site of SO_4^{2-}/ZrO_2-NiO attributes to its mesoporous structure. Fig. 4a illuminated that the amounts of $Ni(NO_3)_2$ adding to SO_4^{2-}/ZrO_2 had a great effect on its catalytic activity and specific surface area was an important factor affecting the catalytic activity of SO_4^{2-} / M_xO_y solid acid.

2.2. Influence of impregnating sulfuric acid concentration

The corresponding conversion with impregnating different acid concentrations was shown in Fig. 4b. The condition of reaction was the same as in the above 3.2.1. When impregnating the concentration of acid was 2.0M, the conversion of n-butyl acetate was the highest, which is consistent with the previous analysis of Sulfur content and TPD.

2.3. Effect of catalyst amount

The influence of catalyst amount on the conversion rate of acetic acid is presented in Fig. 4c. From the figure, it can be noted that the conversion rate of acetic acid increased with higher catalyst amount until a value in which higher increment no longer increased the conversion rate of acetic acid. This is because the esterification of acetic acid and n-butanol is an acid-catalyzed reaction, when the amount of catalyst is small the number of available active sites required for the esterification reaction is insufficient, which results in a lower conversion yield of acetic acid. The conversion rate of acetic acid reached 98% when the amount of catalyst is the quality of acetic acid 2%, and the amount of catalyst was less than that of pure SO_4^{2-}/ZrO_2, which is due to the addition of Ni increased the specific surface area of the solid acid, providing more catalytic active sites to enhance the catalytic activity of the catalyst.

2.4. Influence of molar ratio of reactants

In general, for a reversible reaction like esterification, reactants (acetic acid) are usually used in excess to accelerate the reaction forward for formation of products (*n*-butyl acetate). As thus, care must be taken as to how much acetic acid is to be used because too much acetic acid may weaken the system, eventually cause a drop in the yield of *n*-butyl acetate. Effect of molar ratio of acetic acid to n-butanol on the conversion rate of acetic acid is shown in Fig. 4d. Lots of molar ratios of acetic acid to *n*-butanol were expound during the esterification, which includes 2:1, 1:1, 1:2, 1:3, 1:4, and 1:6. From the figure, the conversion yield of acetic acid catalyzed by SO_4^{2-}/ZrO_2-NiO increased abruptly from 55.0% to 98.0% as the molar ratio of acetic acid to n-butanol decreased from 2:1 to 1:2, then the conversion decreased inconspicuously with the further decrease of molar ratio. Consequently, the optimum molar ratio of acetic acid to n-butanol is 1:2.

2.5. Effect of reaction temperature

The effect of reaction temperature on the esterification was investigated, and the experiments were carried out at 60, 70, 80, 90 °C, respectively. It can be arrived at from Fig. 4e that temperature played an important influence on conversion rate of acetic acid. When the reaction temperature was increased from 60 to 90 °C, there is a gradual increase in the conversion yield of acetic acid, attributing to higher temperature could accelerate the rate of chemical reaction.

2.6. Reusability of the catalyst

Long-term stability of solid acid catalysts is a significantly important characteristic for practical application to reduce production cost. In consideration of good separability and easy recovery of solid acid catalyst, it is necessary to evaluate the reusability of the as-prepared SO_4^{2-}/ZrO_2-NiO catalyst. After the reaction was finished, the spent catalyst was separated from the liquid products, and then used for esterification under the same experimental conditions. After each cycle, the catalyst was recovered by filtration, washed with ethanol, and then reused. As shown in Fig. 5a, for the first two cycles, there was almost no decrease in the activity of the catalyst. In the subsequent four cycles, the conversion rate of acetic acid diminished as increasing the catalyst reuse number. However, in the sixth cycle, the conversion still remained as high as 85.3 %. On the other hand, the XRD patterns of SO_4^{2-} / ZrO_2-NiO after six times cycles were shown in Fig. 5b, it can be seen that the crystal structure of catalyst was almost unchanged after six times repeated application still maintaining the tetragonal phase structure. All these results indicated the good reusability of the as-prepared SO_4^{2-}/ZrO_2-NiO in above esterification.

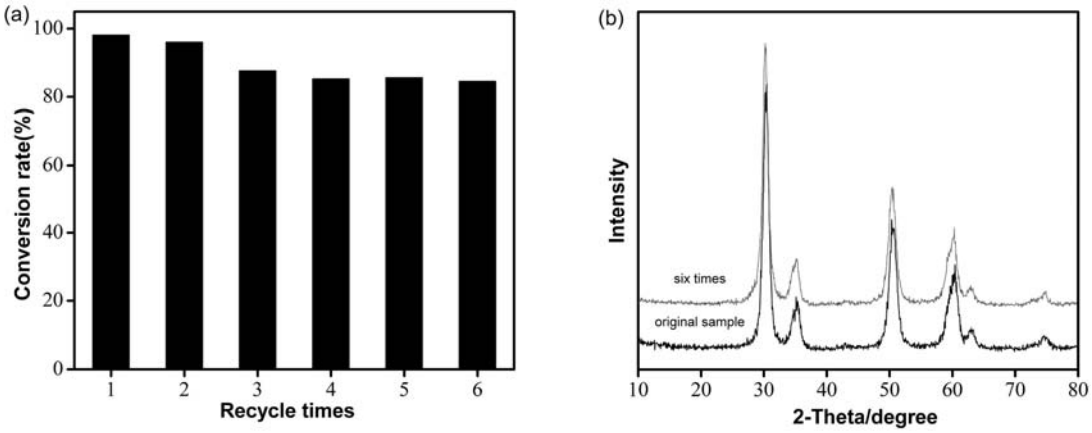

Fig. 5 – Reusability of the catalyst. (a) Reusability of the SO_4^{2-}/ZrO_2-NiO catalyst. (b) XRD patterns of SO_4^{2-}/ ZrO_2-NiO after six times cycles.

CONCLUSION

In conclusion, a facile strategy was developed to synthesize a composite fibrous SO_4^{2-}/ZrO_2-NiO solid superacid catalyst by using collagen fiber as the template. The optimal Preparation conditions of fibrous SO_4^{2-}/ZrO_2-NiO were found out: adding amount of $Ni(NO_3)_2$ was 1.0g, calcination temperature was 500 ^oC, impregnating sulfuric acid concentration was 2.0M. The structure properties of ZrO_2-NiO were examined by XRD, SEM and N_2 adsorption/desorption. The acidity of SO_4^{2-}/ZrO_2-NiO was measured by NH_3-temperature programmed desorption. The consequence of esterification reaction between acetic acid and n-butanol verifies that as-prepared fibrous SO_4^{2-}/ZrO_2-NiO catalyst had high catalytic activity. Furthermore, the catalyst reused 6 times without observably loss of catalytic activity, suggesting satisfied reusability.

Acknowledgements. This work was financially supported by the National Natural Science Foundation of China (21406147, 41641010 and 21506134), the Foundation of Sichuan Science & Technology Committee (2016NZ0053, 2014-HM01-00204-SF). We also thank the support of the Engineering Research Center for the Development of Farmland Ecosystem Service Functions, Sichuan Province Institutions of Higher Education.

REFERENCES

1. C. H. Su, *Appl. Energy*., **2013**, *104*, 503-509.
2. V. Choudhary, A. B. Pinar, R. F. Lobo, D. G. Vlachos and S. I. Sandler, *Chemsuschem*, **2013**, 6, 2369-2376.
3. S. A. Fernandes, R. Natalino, M. J. D. Silva and G. N. Jham, *Tetrahedron Lett*., **2012**, *53*, 1630-1633.
4. A. Corma and H. García, *Chem. Rev*., **2003**, *103*, 4307-4365.
5. J. Lilja, D. Y. Murzin, T. Salmi, J. Aumo, P. Mäki-Arvela and M. Sundell, *Mol. Catal. A: Chem*., **2002**, *182-183*, 555-563.
6. G. Ji, P. Dwivedi, S. Sundaram and R. Prakash, *Ind. Eng. Chem. Res*., **2013**, *52*, 10673-10681.
7. T. F. Parangi, R. M. Patel, U. V. Chudasama and Bull. *Mater. Sci*., **2014**, *37*, 609-615.
8. V. S. Marakatti and A. B. Halgeri, *Rsc. Adv*., **2015**, *5*, 14286-14293.
9. M. Karaki, A. Karout, J. Toufaily, F. Rataboul, N. Essayem and B. Lebeau, *Catal*., **2013**, *305*, 204-216.
10. K. Saravanan, B. Tyagi, R.S. Shukla and H.C. Bajaj, *Appl. Catal. B*., **2015**, *172-173*, 108-115.
11. M. Abdollahi-Alibeik and M. Hajihakimi, *Chem. Pap*., **2013**, *67*, 490-496.
12. K. Saravanan, B. Tyagi and H. C. Bajaj, *Catal. Sci. Technol*., **2012**, *2*, 2512-2520.
13. X. Zhang, J. Long, K. Wei, Q. Zhang, L. Chen, T. Wang, L. Ma and Y. Li, *Energy. Fuels.*, **2014**, *28*, 2562–2570.
14. F. H. Alhassan, U. Rashid and Y. H. Taufiq-Yap, *Fuel*., **2015**, *142*, 38-45.
15. J. M. Hernándezenríquez, R. Silvarodrigo, R. Garcíaalamilla, L. A. Garcíaserrano, B. E. Handy, G. Cárdenasgalindo and A. Cuetohernández, *J Mex. Chem. Soc*., **2012**, *56*, 115-120.
16. D. Bu and H. Zhuang, *Appl. Surf. Sci*., **2013**, *265*, 677-685.
17. Z. Vít, D. Gulková and L. Kaluža, *J. Kupčík, Appl. Catal. B*., **2015**, *179*, 44-53.
18. H. Mao, Y. Shen, Q. Zhang, M. Ulaganathan, S. Zhao, Y. Yang and H. H. Hng, *Carbon*, **2016**, *96*, 75-82.
19. C. Yang, C. H. Choi, C. S. Lee and H. Yi, *Acs Nano*., **2013**, *7*, 5032-5044.
20. B. B. Lakshmi, C. J. P. And and C. R. Martin, *Chem. Mater*., **1997**, *9*, 2544-2550.
21. G. Xiao, X. Huang, X. Liao and B. Shi, *J. Phys. Chem. C*., 2013, *117*, 9739–9746.
22. J. Ma, X. Huang, X. Liao and B. Shi, *J. Mol. Catal. A: Chem*., **2013**, *366*, 8-16.
23. M. M. Yu and M. Sheintuch, *Appl. Catal., A*., **2002**, *231*, 1-16.
24. L. Yang, H. Xin, X. Liao and S. Bi, *J. Mol. Catal. A: Chem*., **2011**, *347*, 46-51.
25. S. J. Han, Y. Bang, J. Yoo, J. G. Seo and I. K. Song, *Int. J. Hydrogen Energy*., **2013**, *38*, 8285-8292.
26. H. Takano, H. Shinomiya, K. Izumiya, N. Kumagai, H. Habazaki and K. Hashimoto, *Int. J. Hydrogen Energy*., **2015**, *40*, 8347-8355.
27. A. G. Sato, D. P. Volanti, D. M. Meira, S. Damyanova, E. Longo and J.M.C. Bueno, *J. Catal*., **2013**, *307*, 1-17.
28. G. Yu, L. Zhu, G. Zhang, G. Qin, H. Fu, F. Ji and J. Zhao, *J. Porous. Mat*., **2014**, *21*, 105-112.
29. M. A. A. Aziz, A. A. Jalil, S. Triwahyono, R. R. Mukti, Y. H. Taufiq-Yap and M. R. Sazegar, *J. Appl. Catal. B*., **2014**, *147*, 359-368.
30. R. Puskás, T. Varga, A. Grósz, A. Sápi, A. Oszkó, Á. Kukovecz and Z. Kónya, *Surf. Sci*., **2016**, *648*, 114-119.